

A Simple Model for Simulating Infiltration in Two-Layer Soil Slope during Unsteady Rainfall and its Application in Slope Stability Analysis

Shaohong Li (✉ lishaohong16@126.com)

Southwest Jiaotong University

Shixin Zhang

Chongqing Three Gorges University

Guoguo Liu

Southwest Jiaotong University

Shuairun Zhu

Chengdu University of Technology

Research Article

Keywords: infiltration, unsteady rainfall, two-layer soil slope, slope stability

Posted Date: July 8th, 2021

DOI: <https://doi.org/10.21203/rs.3.rs-670897/v1>

License:  This work is licensed under a Creative Commons Attribution 4.0 International License.

[Read Full License](#)

1 **A simple model for simulating infiltration in two-layer soil slope**
2 **during unsteady rainfall and its application in slope stability analysis**

3 S. H. Li^{a)*}, S. X. Zhang^{b)}, G.G. Liu^{c*)}, S. R. Zhu^{d)}
4

5 a) Department of Geological Engineering, Southwest Jiaotong University, Chengdu 610031,
6 China

7 b) School of Civil Engineering, Chongqing Three Gorges University, Wanzhou 404100, China

8 c) Key Laboratory of Transportation Tunnel Engineering of Ministry of Education, Southwest
9 Jiaotong University, Chengdu 610031, China

10 d) College of Environment and Civil Engineering, Chengdu University of Technology,
11 Chengdu 610059, China

12 *Corresponding author Email:

13 lishaohong16@126.com (S. H. Li); ldamienrice@my.swjtu.edu.cn (G.G. Liu);

14 Submitted on June 29, 2021

15

Abstract

16
17
18
19
20
21
22
23
24
25
26
27
28
29
30

Based on the Darcy's law and water balance principle, some infiltration models have been proposed, but most of these models are not suitable for simulating infiltration into layered soils during unsteady rainfall. In this paper, a simple model for simulating water infiltration into the two-layer soil slopes during unsteady rainfall was proposed, combined with the limit equilibrium method to analyze the stability of the two-layer soil slope. The water infiltration rate of slopes depends on rainfall intensity and the actual infiltration capacity of soils. The proposed model has been successfully applied to three cases (steady rainfall and homogeneous slope, unsteady rainfall and homogeneous slope, unsteady rainfall and two-layer soil slope), and it can be also combined with probabilistic methods to calculate the failure probability of slopes. Compared with the Richards model, the combination of the proposed model and the random field method can quickly obtain the failure probability of the slope.

Keywords: infiltration; unsteady rainfall; two-layer soil slope; slope stability

31 **1 Introduction**

32 Water infiltration in soils is an important issue in Geological Engineering and Soil Science
33 (Collins and Znidarcic 2004; Tang et al. 2015). The Green-Ampt model, proposed by Green
34 and Ampt (1911), is a fundamental mathematical model to describe the infiltration process. Due
35 to its simplicity, it has received widespread attention. A modified model reflecting the
36 relationship between rainfall intensity and infiltration capacity was proposed by Mein and
37 Larsen (1973). Barry et al. (2005) gave some approximate solutions of Green-Ampt model,
38 which are useful for engineering applications. Based on the numerical solutions of Richards
39 equation, an improved Green-Ampt model that can take into account the effect of groundwater
40 levels was developed by Liu (2013). Considering the relationship between rainfall intensity and
41 infiltration capacity, an explicit solution to Green-Ampt model was developed by Almedeij and
42 Esen (2014). The application range of Green-Ampt model was extended from homogeneous to
43 layered soils by Deng and Zhu (2016). An improved Green-Ampt model considering capillary
44 pressure was proposed by Zhang et al. (2019). Considering the piston assumption of Green-
45 Ampt model simplifies the moisture distribution and overestimates the value, Mao et al. (2016)
46 proposed a method to modify the Green-Ampt model by the amount of soil infiltration. The
47 above (i.e., Mein and Larsen's model, Liu's model, Almedeij and Esen's model, Deng and
48 Zhu's model, Zhang's model, and Mao's model) are modified Green-Ampt models based on
49 physical concepts. Different from these studies, a fractional form of the Green-Ampt model,
50 which introduced a new operation rule, was written by Voller (2011). This approach was cited
51 by Fernández-Pato et al. (2018).

52 However, most of the published studies focus on the infiltration in horizontal soils,

53 increasing attention has been paid from geotechnical engineers to the infiltration in soil slopes,
54 which affects the slope stability and then induces geological disasters (Tsaparas et al. 2002; Liu
55 et al. 2014; Zhang et al. 2017). Green-Ampt model has been gradually applied to slope
56 infiltration during rainfall. For example, a Green-Ampt model for slopes was proposed based
57 on coordinate transformation (Chen and Young 2006); The Green-Ampt model and infinite
58 slope model were used to evaluate the stability of landslides in Italy (Muntohar and Liao 2010);
59 A laboratory test was used to evaluate the accuracy of a new Green-Ampt model, and then a
60 landslide stability assessment method based on the new model and the infinite slope model was
61 also developed (Wu et al. 2018); A novel Green-Ampt model considering the effect of slope
62 length was proposed (Wang et al. 2017).

63 Although the above models have certain applicability, they are not suitable for simulating
64 the infiltration into layered soils during unsteady rainfall. However, rainfall is not uniform and
65 most of slopes are inhomogeneous on the earth (Alcantara-Ayala 2004; Dai et al. 2002). The
66 schematic diagram of rainfall infiltration into a two-layer slope is shown in Fig.1. Due to the
67 unsteady of rainfall and the differences of soil physical and mechanical parameters in different
68 layers, it is difficult to study the infiltration behavior of water in the two-layer soil slope. Some
69 methods for analyzing the infiltration in two-layer soil slopes have been developed. For
70 example, Zhan et al. (2013) obtained an analytical solution of Richards' equation for describing
71 rainfall infiltration by Laplace transform; De Luca and Cepeda (2016) developed a simple
72 program to solve the Richards' equation for a two-layer soil slope; Wu et al. (2020) obtained an
73 analytical solution of infiltration of two-layer soil slope considering hydraulic coupling; Zhu et
74 al. (2020) proposed an improved Chebyshev semi-iterative method to analyze the infiltration

75 process of water in the two-layer slope. Unfortunately, these methods were obtained by solving
76 the Richards equation. Although they are more completed in theory, its application in actual
77 engineering is limited due to the complicated mathematical expression and they are only used
78 in the case of uniform rainfall. Cho (2009) proposed a method for analyzing two-layer slope
79 infiltration during steady rainfall based on an improved Green-Ampt model, however, this
80 method did not consider the impact of slope angle on infiltration.

81 This paper aims to develop an approach to simulate the water infiltration behavior in two-
82 layer slopes during unsteady rainfall. The rest of this paper is organized as follows:

83 Section 2 introduces the proposed model. Section 3 are three numerical cases. Section 4 is
84 the discussions. The conclusions are drawn in the end.

85 **2 Model**

86 **2.1 Infiltration rate of water in soil slopes**

87 The infiltration rate of water in soil slopes depends on rainfall intensity and soil infiltration
88 capacity (soil infiltration capacity is determined by Darcy's law (Hillel 1980)). The slope
89 infiltration rate determined by the rainfall intensity can be expressed as:

$$90 \quad i_1 = q_{rain} \cos \alpha \quad (1)$$

91 where, α represents the slope angle (Fig. 1). The cumulative infiltration volume I can be
92 expressed as:

$$93 \quad I = z_f \Delta \theta \quad (2)$$

94 where, z_f represents the wetting front depth (the wetting front refers to the interface between the
95 saturated zone and the natural zone as shown in Fig. 2); $\Delta \theta$ represents the difference of the
96 saturated moisture content(θ_{sat}) and the natural moisture content(θ_i) of soil. According to Eqs.(1)

97 and (2), the following relationship is established:

$$98 \quad \frac{dI}{dt} = i_1 \Leftrightarrow \frac{dz_f}{dt} = \frac{q_{rain} \cos \alpha}{\Delta \theta} \quad (3)$$

99 according to Eq.(3), the relationship between the wetting front depth and time (t) can be
100 obtained as:

$$101 \quad z_f = i_1 t / \Delta \theta \quad (4)$$

102 The infiltration rate determined by soil infiltration capacity can be expressed as (i.e.,
103 Darcy's law):

$$104 \quad i_2 = k_s \left(\frac{z_f \cos \alpha + h_f}{z_f} \right) \quad (5)$$

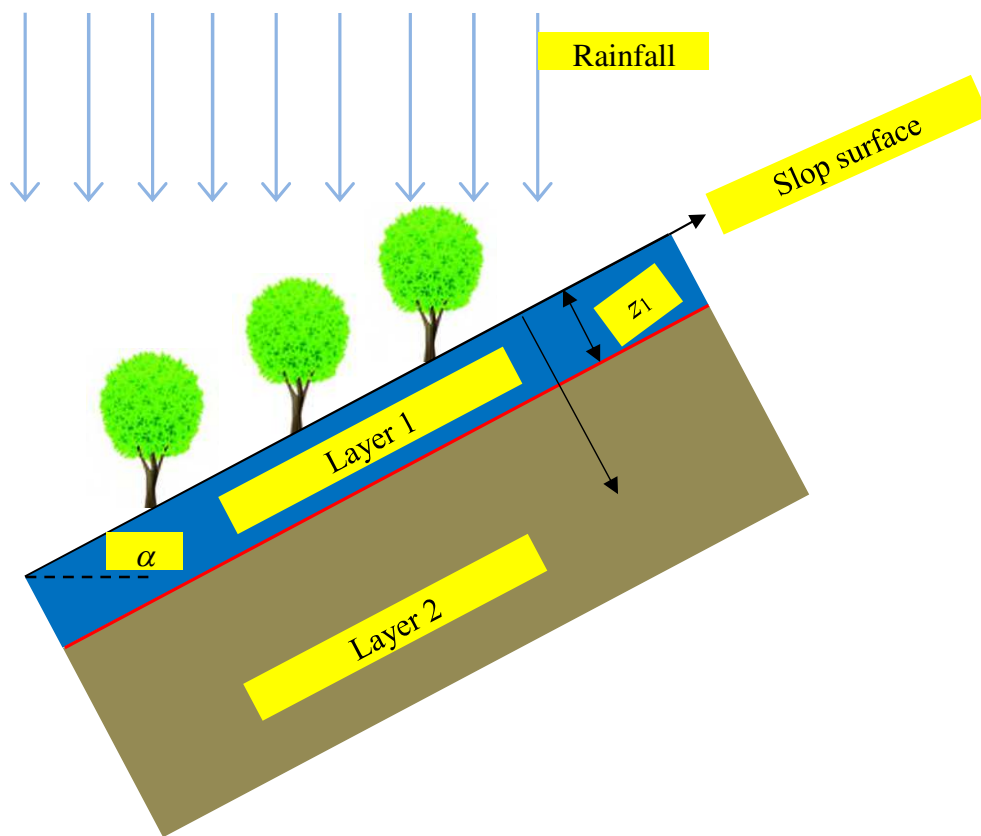
105 where, k_s represents the saturated permeability coefficient of soil; h_f represents the matrix
106 suction head. According to Eq.(5), the relationship between the wetting front depth and time
107 can be obtained as:

$$108 \quad \frac{dz_f}{dt} = \frac{i_2}{\Delta \theta} \quad (6)$$

109 The infiltration rate of water in soils should be the minimum value between i_1 and i_2 , i.e.,

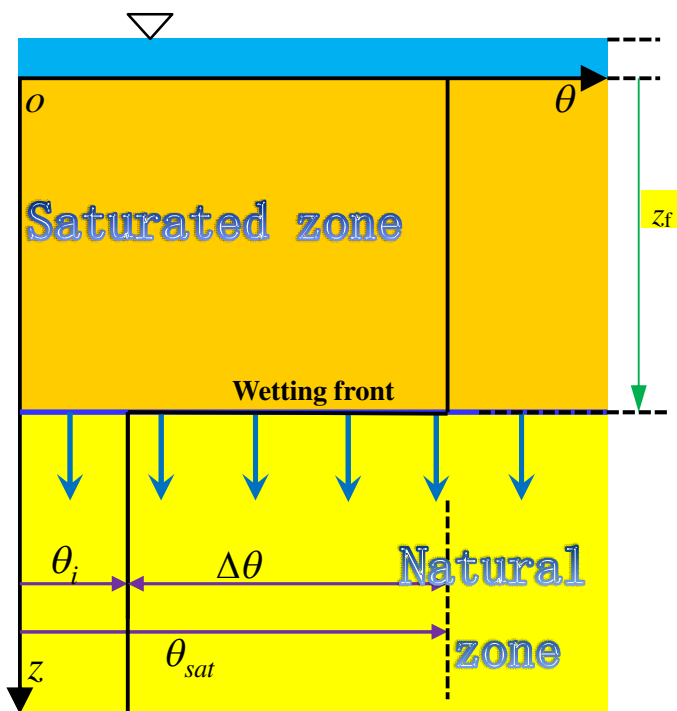
$$110 \quad i = \min \{i_1, i_2\} \quad (7)$$

111 It should be noted that the above derivations all assume that there would be no ponding on the
112 soil surface (Wu et al. 2018).



113

114 **Fig. 1** Infiltration in a soil slope during rainfall



115
116

Fig.2 Infiltration behavior of water in the soil

117 **2.2 Simulation of water infiltration in two-layer soil slopes**

118 Let me rewrite Eqs.(4) and (6) into a discretize form ($t = \{0, \Delta t, 2\Delta t, K, i\Delta t, K\}$):

119
$$z_{f,i} = z_{f,i-1} + i_1 \Delta t / \Delta \theta_1 \quad (8)$$

120
$$z_{f,i} = z_{f,i-1} + \frac{i_2}{\Delta \theta_1} \Delta t \quad (9)$$

121 where, $z_{f,i}$ represents the wetting front depth corresponding to time $i\Delta t$ ($z_{f,0} = 0$). To facilitate
 122 the distinction, record the saturated permeability coefficient of the layer 1 (Fig. 1) of soil as k_{s1} ,
 123 and the suction head is denoted as h_{f1} , and the difference of moisture content is $\Delta \theta_1$. According
 124 to Eqs.(8) and (9), the wetting front depth vs. time in the layer 1 of soil can be obtained. After
 125 water penetrating into the layer 2 of soil ($z_f > z_1$, z_1 represents the depth of layer 1), the
 126 infiltration rate determined by the soil infiltration capacity can be expressed as:

127
$$i_2 = \frac{z_f \cos \alpha + h_{f2}}{\frac{z_1}{k_{s1}} + \frac{z_f - z_1}{k_{s2}}}, z_f > z_1 \quad (10)$$

128 where, k_{s2} represents the saturated permeability coefficient of layer 2, while h_{f2} represents the
 129 matrix suction head of layer 2. The derivation of Eq.(10) can be found in the Appendix. Then
 130 the wetting front depth can be expressed as follows:

131
$$z_{f,i} = z_{f,i-1} + i_1 \Delta t / \Delta \theta_2 \quad (11)$$

132
$$z_{f,i} = z_{f,i-1} + \frac{i_2}{\Delta \theta_2} \Delta t \quad (12)$$

133 where, $\Delta \theta_2$ represents the difference of saturated moisture content and natural moisture content
 134 of layer 2.

135 The flow chart of simulating infiltration of water in the two-layer soil can be seen in Fig.

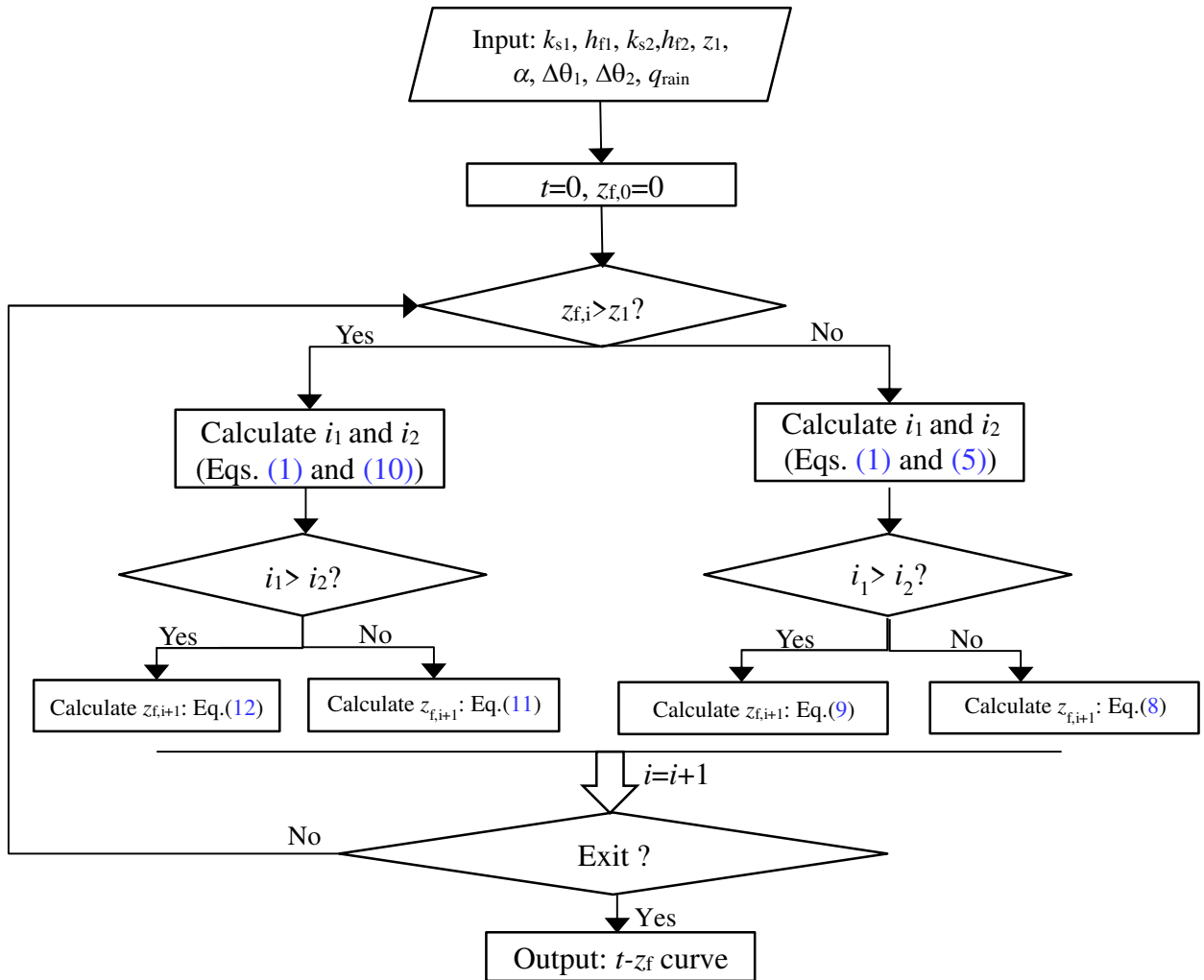
136 3. The core of the proposed model is to use difference calculation instead of differential

137 calculation. According to the proposed model, it is easy to simulate the infiltration of water in
 138 two-layer soil slopes during unsteady rainfall.

139 Combined with the limit equilibrium method, the slope safety factor (F_s) can be expressed
 140 as (the wetting front is slip surface) (Zhu et al. 2020):

$$141 \quad F_s = \frac{c + (\gamma z_f \cos^2 \alpha - \gamma_w z_f \cos^2 \alpha) \tan \varphi}{\gamma z_f \cos \alpha \sin \alpha} \quad (13)$$

142 where, γ and γ_w represent the unit weight of soil and water, c and φ represent cohesion and
 143 internal friction angle. The numerator term of Eq.(13) is also called anti-sliding force, and the
 144 denominator term is called sliding force. By substituting Eqs.(8)-(12) into Eq.(9), the slope
 145 safety factor at any time can be obtained.



146

147 **Fig.3** The flow chart of the proposed model

148 **3 Numerical cases**

149 In this section, to facilitate the distinction, record unit weight, cohesion and internal friction
150 angle of the layer 1 as γ_1 , c_1 and φ_1 , respectively, these of layer 2 are denoted as γ_2 , c_2 and φ_2 ,
151 respectively. In the following three cases, $\Delta t = 5$ min. The calculation results in this paper were
152 obtained through MATLAB software (Mathworks 2018a).

153 **3.1 Case 1: steady rainfall and homogeneous slope**

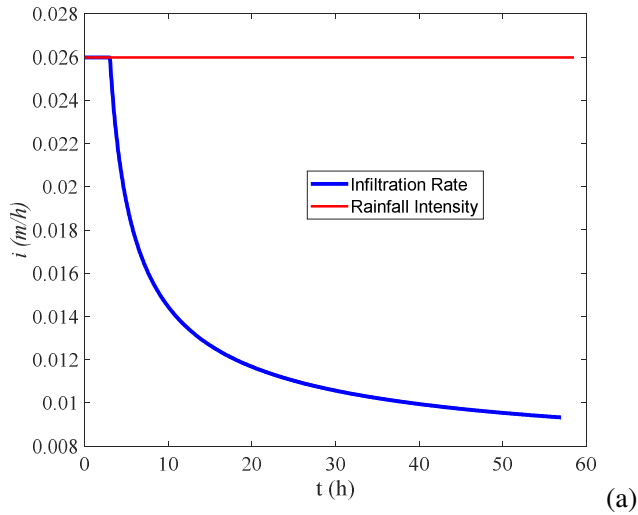
154 The calculation parameters are shown in Table 1.

155 **Table 1** Calculation parameters of Case 1

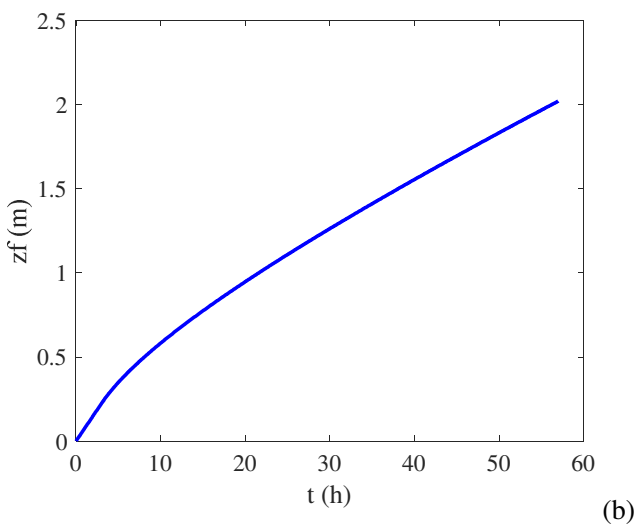
$\Delta\theta_1$	q_{rain} (m/h)	h_{f1} (m)	k_{s1} (m/h)	α (deg.)	c_1 (kPa)	φ_1 (deg.)	γ (kN/m ³)
0.35	0.03	0.5	0.00837	30	13.5	36	19.2

156

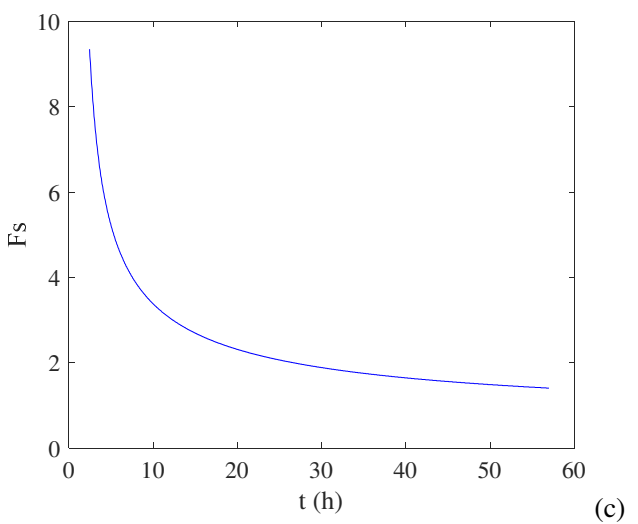
157 Figure 4(a) shows the variation of infiltration rate over time, and we can conclude that the
158 infiltration rate determined by rainfall intensity ($q_{\text{rain}}\cos\alpha$) at the beginning of precipitation,
159 while it is determined by infiltration capacity in the later period of precipitation. The wetting
160 front depth vs. time curve is shown in Fig. 4(b). With the decrease of infiltration rate, the
161 forward rate of the wetting front decreases gradually. Figure 4(c) is the safety factor during
162 rainfall. With the increase of rainfall duration, the slope safety factor reduces, indicating that
163 rainfall has a negative influence on the slope stability.



164



165



166

167 **Fig.4** The calculation results of Case 1: (a) rainfall intensity and infiltration rate of water in
 168 soils, (b) the wetting front depth vs. time curve, and (c) the safety factor during rainfall

169 There is an analytical solution to obtain the wetting front of slopes (Chen and Young 2006):

$$\begin{cases} t = z_f \Delta\theta_1 / (q_{rain} \cos \alpha), z_f < z_p \\ t = t_p + A_1 + A_2, z_f \geq z_p \end{cases} \quad (14a)$$

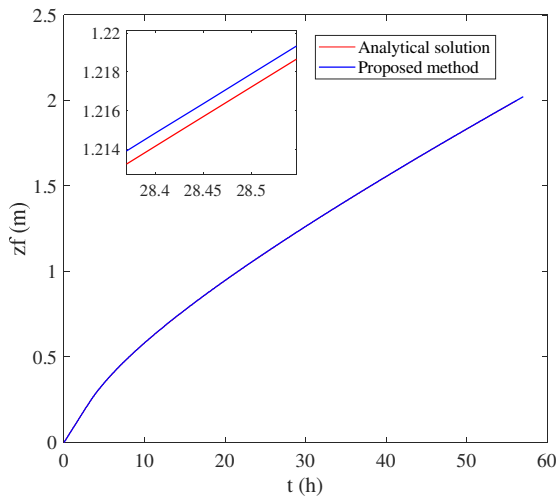
171 where,

$$\begin{cases} A_1 = \Delta\theta_1 (z_f - q_{rain} \cos \alpha t_p) / k_{s1} \cos \alpha \\ A_2 = (\Delta\theta_1 (-h_{f1}) \ln(h_{f1} - z_f \cos \alpha / h_{f1} - q_{rain} \cos^2 \alpha t_p)) / k_{s1} \cos^2 \alpha \end{cases} \quad (14b)$$

$$z_p = \frac{h_{f1}}{(q_{rain} / k_{s1} - 1) \cos \alpha} \quad (14c)$$

$$t_p = \frac{\Delta\theta_1 z_p}{q_{rain} \cos \alpha} \quad (14d)$$

175 Figure 5 compares the results of Eq. (14) with that of the proposed model. As shown in
 176 Fig. 5, the results of the proposed model are almostly consistent with that of Eq. (14), which
 177 verifies the reasonability and practicability of the proposed method.



178
 179 **Fig.5** Results of the proposed model and Eq. (14)

180 3.2 Case 2: unsteady rainfall and homogeneous slope

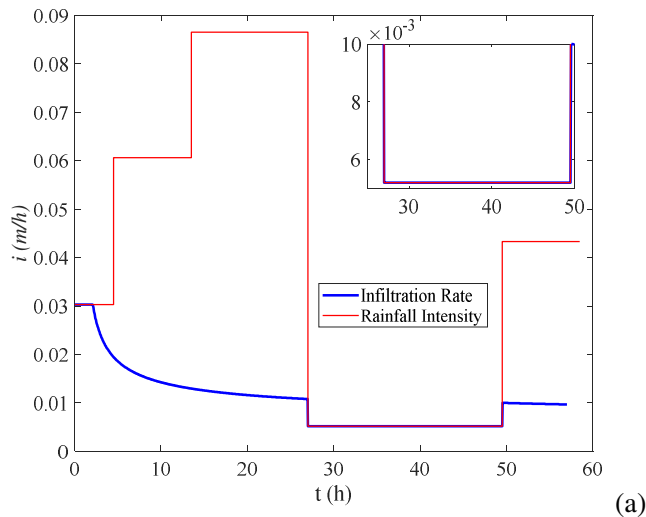
181 The calculation parameters are shown in Table 2.

182 **Table 2** Calculation parameters of Case 2

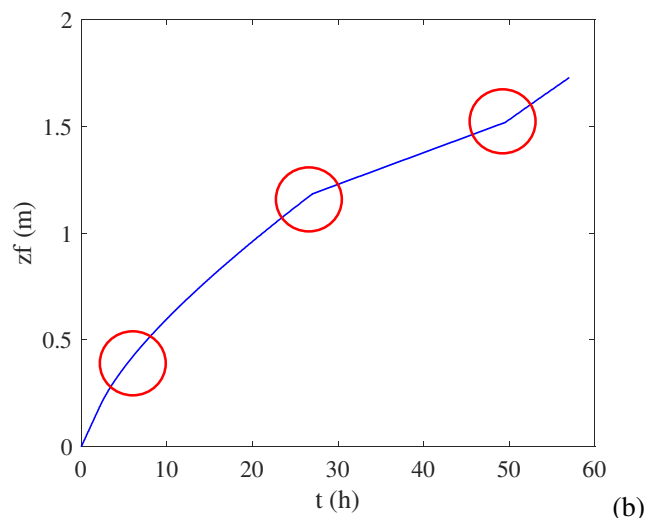
$\Delta\theta_1$	h_{f1} (m)	k_{s1} (m/h)	α (deg.)	c_1 (kPa)	φ_1 (deg.)	γ_1 (kN/m ³)
0.35	0.5	0.00837	30	13.5	36	19.2

183

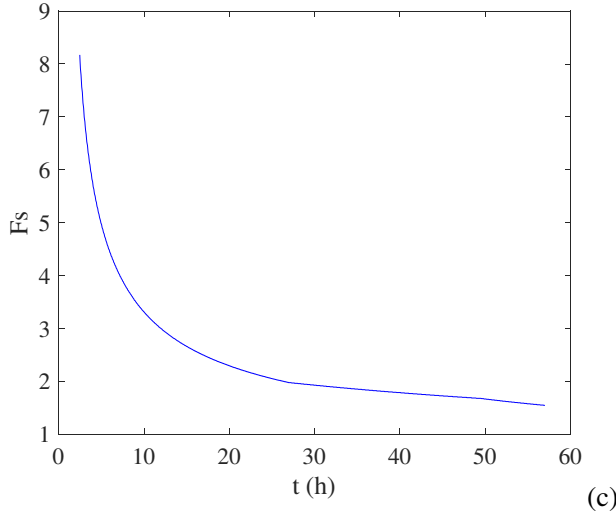
184 Figure 6(a) is the variation of infiltration rate and rainfall intensity over time. Rainfall
 185 intensity has a great impact on infiltration rate. And the infiltration rate would be converted
 186 between rainfall intensity and soil infiltration capacity with the variation of rainfall intensity.
 187 Figure6(b) shows the variation of wetting front. Due to the variation of rainfall intensity, it can
 188 be seen that there are many turning points in the forward curve of wetting front. Compared with
 189 Case 1, the wetting front decreases. Figure6(c) is the variation of the safety factor. As rainfall
 190 duration increases, the safety factor decreases gradually. Since the wetting front depth in Case
 191 2 is less than that in Case 1, the safety factor of Case 2 is larger.



192 (a)



193 (b)



194

195 **Fig.6** The calculation results of Case 2: (a) rainfall intensity and infiltration rate of water in soil,
 196 (b) the wetting front vs. time curve, and (c) the safety factor during rainfall

197 From this case we can learn that rainfall intensity has a great affection on infiltration
 198 behavior. Rainfall intensity is unsteady in actual. However, many infiltration models simplify
 199 non-uniform rainfall intensity to uniform rainfall intensity, which may result in a nonnegligible
 200 difference (e.g., Muntohar and Liao 2010; Zhang et al., 2017; Wu et al. 2018).

201 **3.3 Case 3: unsteady rainfall rainfall and two-layer slope**

202 The calculation parameters are shown in Table 3.

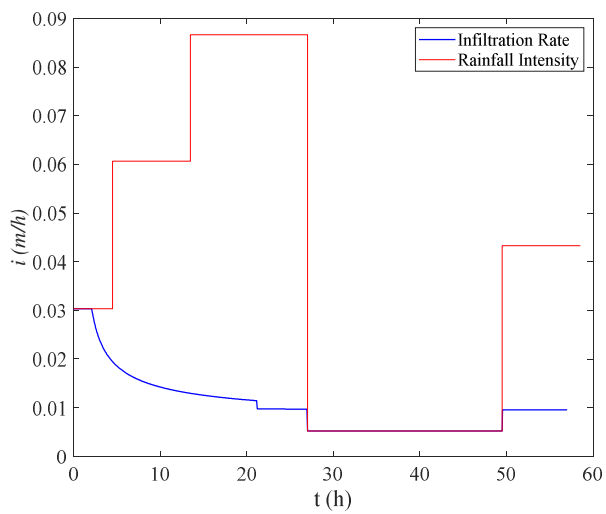
203 **Table 3** Calculation parameters of Case 3

layer 1	value	layer2	value
$\Delta\theta_1$	0.35	$\Delta\theta_2$	0.45
h_{f1} (m)	0.5	h_{f2} (m)	0.3
k_{s1} (m/h)	0.00837	k_{s2} (m/h)	0.01037
α (deg.)	30	α (deg.)	30
c_1 (kPa)	13.5	c_2 (kPa)	10.5
φ_1 (deg.)	36	φ_2 (deg.)	30
γ_1 (kN/m ³)	19.2	γ_2 (kN/m ³)	18
z_1 (m)	1		

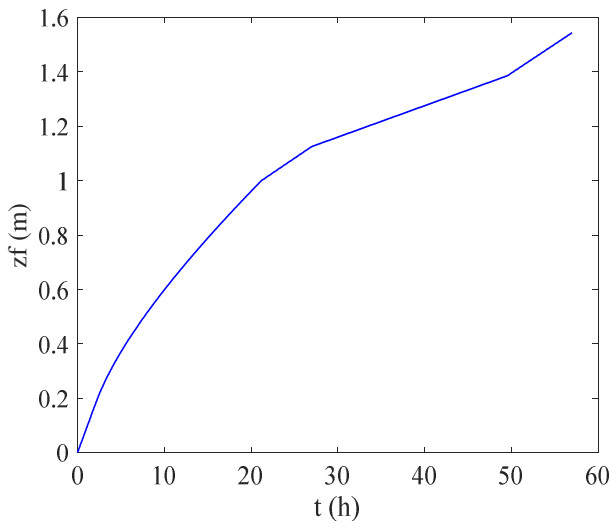
204

205 Figure 7(a) is the variation of infiltration rate and rainfall intensity over time. Different
 206 from Case 2, besides rainfall intensity, the difference of soil parameters between two soil layers
 207 also affects the infiltration rate. With the variation of rainfall intensity, infiltration rate would

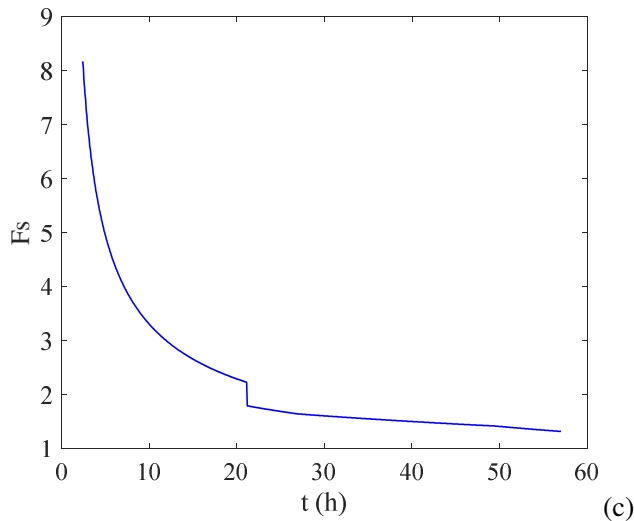
208 be converted between rainfall intensity and soil infiltration capacity. About 20h later, when
209 rainfall penetrates into the second layer, the infiltration rate decreases suddenly. Figure7(b)
210 shows the variation of wetting front , compared with that in Case 2, wetting front depth is further
211 reduced. Figure 7(c) is the variation of the slope safety factor during rainfall. Due to the
212 differences in weight, cohesion, and internal friction angle between two soil layers, the safety
213 factor decreases suddenly when water penetrates into the second layer.



214 (a)



215 (b)



216

217 **Fig.7** The calculation results of Case 3: (a) rainfall intensity and infiltration rate of water in soil,
 218 (b) the wetting front depth vs. time curve, and (c) the safety factor during rainfall

219 Case 3 indicates that in addition to rainfall intensity, the differences of physical and
 220 mechanical parameters between two layers of soil have a great influence on the infiltration
 221 behavior of water.

222 4 Discussions

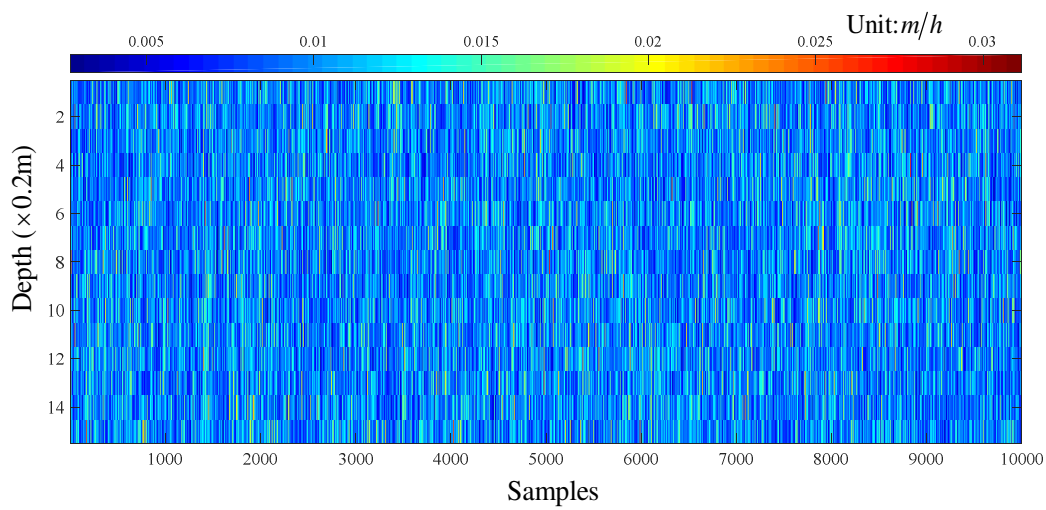
223 a) Failure probability analysis of slopes based on the proposed model

224 The proposed model can also be used to solve the infiltration problem of multilayer soils
 225 (see Appendix) and combined with the probability analysis method to perform the failure
 226 probability analysis of the slope (Johari and Fooladi 2020).

227 By treating the saturated permeability coefficient as a spatial random variable (also known
 228 as a random field), the uncertainty analysis in the infiltration process can be performed. The
 229 random field of saturation coefficient can be generated by Cholesky decomposition method
 230 (Haldar and Sivakumar 2008; Kasama and Whittle 2011). Remember that the number of
 231 random fields generated is N , where the safety factor is less than 1 and the number is N_1 , then
 232 the failure probability of the slope is defined as:

233
$$P_f = \frac{N_1}{N} \times 100\% \quad (15)$$

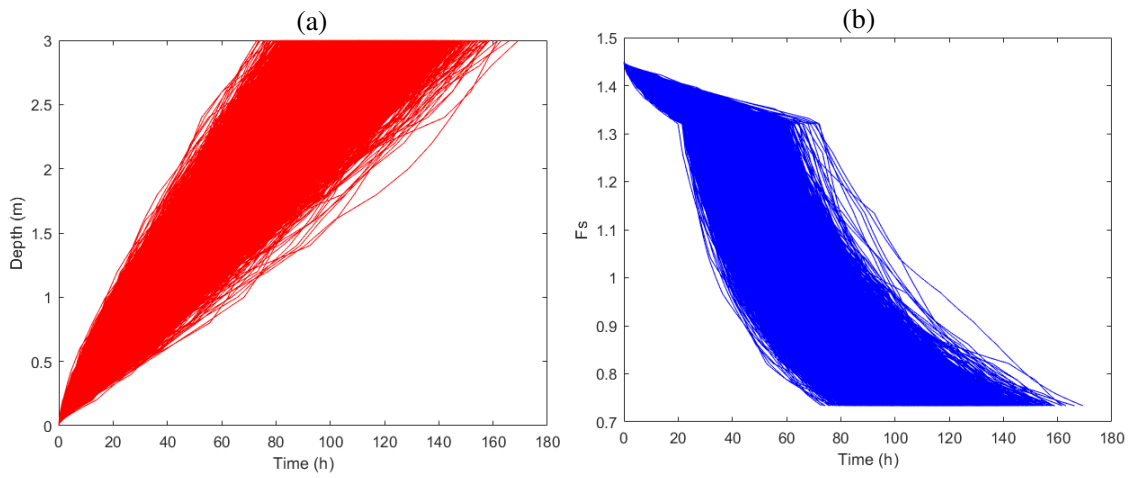
234 Figure 8 is a random field of 10,000 samples generated when the mean value of the
 235 permeability coefficient is 0.01m/h, the coefficient of variation is 0.3, and the autocorrelation
 236 distance is 0.2m. Since the saturated permeability coefficient is a function of depth, it is
 237 necessary to use an infiltration model suitable for multi-layered soil (e.g., proposed model) to
 238 obtain the failure probability of the slope.



239
 240 **Fig.8** Samples of saturated permeability coefficient

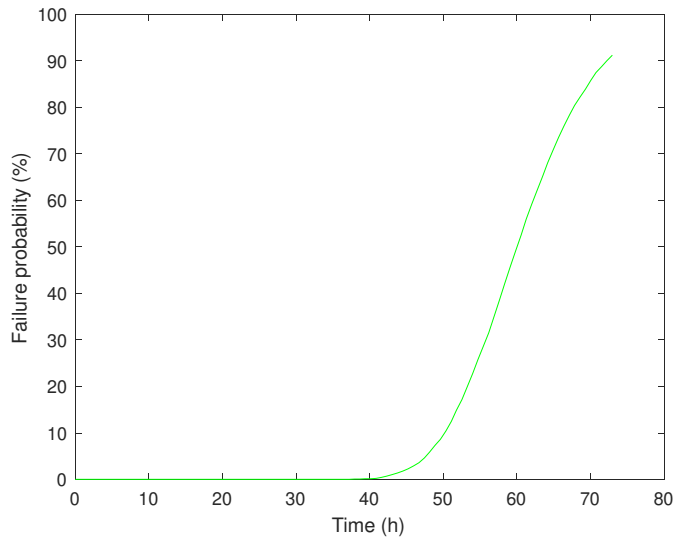
241 Assume that the soil cohesion is 10kPa and the internal friction angle is 25 degrees. It
 242 should be noted that cohesion and internal friction angle are not regarded as spatial random
 243 variables in this paper for simplification. In addition, when the cohesion and internal friction
 244 angle are constant, the minimum safety factor of the slope can be obtained only by taking the
 245 minimum value of the safety factor at the wetting front and the bedrock surface. According to
 246 Fig. 8, the wetting front vs. time curve (Fig. (9a)) and the safety factor vs. time curve (Fig.(9b))
 247 under 10,000 samples were obtained. The failure probability vs. time curve is shown in Fig. 10.
 248 The results show that in the first 40 hours, the slope has almost no possibility of instability, and

249 after about 60 hours, the failure probability of the slope almost exceeds 50%.



250

251 **Fig.9** (a) Wetting front depth-time curve and (b) safety factor-time curve



252

253 **Fig. 10** Slope failure probability during rainfall

254 Although Dou et al. (2015) has developed a stability uncertainty method for shallow slopes,
255 it requires solving the Richards equation, which is extremely time-consuming. Using the
256 proposed model to perform uncertain analysis of shallow slopes has the advantages of
257 convenience and speed.

258 **b) Limitations of the proposed model**

259 Since the moisture in soils is redistributed after rainfall stops, the proposed model cannot
260 be applied to simulate the infiltration of water in soils under the condition of intermittent rainfall.

261 Besides, the proposed method did not take into account the unsaturated infiltration
262 characteristics of soils. In future works, the proposed model can also be combined with
263 advanced probability analysis methods to calculate the failure probability of slopes. When
264 performing slope failure probability analysis, the uncertainty of saturated permeability
265 coefficient and soil strength parameters (cohesion and internal friction angle) should be
266 considered.

267 **5 Conclusions**

268 The conclusions are drawn as follows:

269 (1) A simple model for analyzing the infiltration behavior in two-layer soil slopes during
270 unsteady rainfall was proposed. The results of the proposed model are almostly consistent with
271 that of the existing analytical models under the condition of steady rainfall and homogeneous
272 soil slope.

273 (2) The actual infiltration rate of water is the minimum value of rainfall intensity and the
274 actual infiltration capacity of soils. The differences in unit weight, cohesion, and internal
275 friction angle between two soil layers affect the slope stability.

276 (3) The proposed model can be combined with probabilistic methods to calculate the
277 failure probability of slopes. Moreover, compared with the existing methods of rainfall and
278 landslide probability analysis, the proposed model highlights convenience and less calculation
279 time.

280 Future work is to combine the proposed model with advanced probability analysis methods
281 to calculate the failure probability of slopes.

282 **Appendix**

283 **Derivation Eq .(10)**

284 As shown in Fig. 1, after water penetrating into the second layer, the uniform rate of
 285 wetting front can be expressed as:

$$286 \quad i_2 = k_{s1} \frac{H_0 - H_1}{z_1} = k_{s2} \frac{H_1 - H_{z_f}}{z_f - z_1} \quad (15)$$

287 where, H_0 represents the head height of slope surface, while H_1 represents the head height of
 288 the contact surface of two layers of soil and H_{z_f} represents the head height at wetting front,
 289 and there have:

$$290 \quad \begin{cases} H_0 = 0 \\ H_{z_f} = z_f \cos \alpha + h_{f2} \end{cases} \quad (16)$$

291 Substituting Eq.(16) into Eq.(15) leads to:

$$292 \quad H_1 = - \frac{k_{s2} \frac{z_f \cos \alpha + h_{f2}}{z_f - z_1}}{\frac{k_{s1}}{z_1} + \frac{k_{s2}}{z_f - z_1}} \quad (17)$$

293 We can obtain Eq.(10) by substituting Eq.(17) into Eq.(15).

294 In fact, if soil slope more than two layers, in the n th layer of soil, the infiltration rate
 295 determined by soil infiltration capacity can be expressed as:

$$296 \quad i_n = \frac{z_f \cos \alpha + h_{fn}}{\sum_{j=1}^{n-1} \frac{z_j - z_{j-1}}{k_{sj}} + \frac{z_f - z_{n-1}}{k_{sn}}} \quad (18)$$

297 where, k_{sj} represents the saturated permeability coefficient of the j th layer of soil, and h_{fn}
 298 represents the suction head of the n th layer soil and z_j represents the height of the j th layer of
 299 soil.

300 **Acknowledgments**

301 We thank the National Natural Science Foundation of China (no. 41672282) and the National
302 Key Research and Development Program of China (no. 2018YFC1504702).

303 **Data availability**

304 All data generated or analyzed during this study are included within the article.

305 **Conflict of interest**

306 The authors declare that they have no conflict of interest.

307

308 **References**

309 Alcantara-Ayala I. (2004). Hazard assessment of rainfall-induced landsliding in Mexico.

310 *Geomorphology* 61(1-2) 19–40.

311 Almedeij J, Esen II. (2014). Modified Green-Ampt infiltration model for steady rainfall.

312 *Journal of Hydrologic Engineering* 19(9) 04014011.

313 Barry DA, Parlange JY, Li L, Jeng DS, Crapper M. (2005). Green–Ampt approximations.

314 *Advances in Water Resources* 28(10) 1003-1009.

315 Chen L, Young MH. (2006). Green-ampt infiltration model for sloping surfaces. *Water*

316 *Resources Research* 42(7) 887 - 896.

317 Cho SE. (2009). Infiltration analysis to evaluate the surficial stability of two-layered slopes

318 considering rainfall characteristics. *Engineering Geology* 105(1-2) 32–43.

319 Collins BD, Znidarcic D. (2004). Stability analyses of rainfall induced landslides. *Journal of*

320 *Geotechnical and Geoenvironmental Engineering* 130 (4) 362–372.

321 Dai FC, Lee CF, Ngai YY. (2002). Landslide risk assessment and management: an overview.

322 *Engineering Geology* 64(1) 65–87.

323 Deng P, Zhu JT. (2016). Analysis of effective Green–Ampt hydraulic parameters for vertically
324 layered soils. *Journal of Hydrology* 538 705-712.

325 De Luca DL, Cepeda JM. (2016). Procedure to obtain analytical solutions of one-dimensional
326 Richards’ equation for infiltration in two-layered soils. *Journal of Hydrologic Engineering*
327 21(7) 04016018.

328 Dou HQ, Han TC, Gong XN, Zhang J. (2014). Probabilistic slope stability analysis considering
329 the variability of hydraulic conductivity under rainfall infiltration–redistribution
330 conditions. *Engineering Geology* 183 1–13.

331 Dou HQ, Han TC, Gong XN, Qiu Z, Li Z. (2015). Effects of the spatial variability of
332 permeability on rainfall-induced landslides. *Engineering Geology* 192 92–100.

333 Fernández-Pato J, Gracia JL, García-Navarro P. (2018). A fractional-order infiltration model to
334 improve the simulation of rainfall/runoff in combination with a 2D shallow water model.
335 *Journal of Hydroinformatics* 20(4) 898-916.

336 Green WH, Ampt GA. (1911). Studies on soil physics. *The Journal of Agricultural Science* 4(1)
337 1-24.

338 Haldar S, Sivakumar BGL. (2008). Effect of soil spatial variability on the response of laterally
339 loaded pile in undrained clay. *Computers and Geotechnics* 35(4) 537–547.

340 Hillel D. (1980). Fundamentals of soil physics. Academic Press, New York, NY.

341 Johari A, Fooladi H. (2020). Comparative study of stochastic slope stability analysis based on
342 conditional and unconditional random field. *Computers and Geotechnics* 125 103707.

343 Kasama K, Whittle AJ. (2011). Bearing capacity of spatially random cohesive soil using

344 numerical limit analysis. *Journal of Geotechnical and Geoenvironmental Engineering*,
345 *ASCE* 137(11) 989–996.

346 Liu EL, Yu HS, Deng G, Zhang JH, He SM. (2014). Numerical analysis of seepage–deformation
347 in unsaturated soils. *Acta Geotechnica* 9 1045–1058.

348 Liu GX, Craig JR, Soulis ED. (2011). Applicability of the Green-Ampt infiltration model with
349 shallow boundary conditions. *Journal of Hydrologic Engineering* 16(3) 266-273.

350 Mao LL, Li Y, Hao W, Zhou X, Xu C, Lei T. (2016). A new method to estimate soil water
351 infiltration based on a modified Green–Ampt model. *Soil and Tillage Research* 161 31-37.

352 Mathworks. (2018a). MATLAB Version 9.4.0. The Mathworks, Inc. Natick, Massachusetts.

353 Mein RG, Larson CL. (1973). Modeling infiltration during a steady rain. *Water Resources*
354 *Research* 9(2) 384–394.

355 Muntohar AS, Liao HJ. (2010). Rainfall infiltration: infinite slope model for landslides
356 triggering by rainstorm. *Natural Hazards* 54 967–984.

357 Voller VR. (2011). On a fractional derivative form of the Green–Ampt infiltration model.
358 *Advances in Water Resources* 34(2) 257-262.

359 Wang DJ, Tang HM, Zhang YH, Li CD, Huang L. (2017). An improved approach for evaluating
360 the time-dependent stability of colluvial landslides during intense rainfall. *Environmental*
361 *Earth Sciences* 76 321.

362 Wu LZ, Zhang LM, Zhou Y, Xu Q, Yu B, Liu GG, Bai LY. (2018). Theoretical analysis and
363 model test for rainfall-induced shallow landslides in the red-bed arearegion of Sichuan.
364 *Bull Eng Geol Environ* 77 1343–1353.

365 Wu LZ, Huang JS, Fan W, Li X. (2020). Hydro-mechanical coupling in unsaturated soils

366 covering a non-deformable structure. *Computers and Geotechnics* 117 103287.

367 Tang YM, Xue Q, Li ZG, Feng W. (2015). Three modes of rainfall infiltration inducing loess
368 landslide. *Natural Hazards* 79 137–150.

369 Tsaparas I, Rahardjo H, Toll D, Leong E. (2002). Controlling parameters for rainfall-induced
370 landslides. *Computers and Geotechnics* 29(1) 1–27.

371 Zhang S, Xu Q, Zhang Q. (2017). Failure characteristics of gently inclined shallow landslides
372 in Nanjiang, southwest of China. *Engineering Geology* 217 1-11.

373 Zhan TLT, Jia GW, Chen YM, Fredlund DG, Li H. (2012). An analytical solution for rainfall
374 infiltration into an unsaturated infinite slope and its application to slope stability analysis.
375 *International Journal for Numerical and Analytical Methods in Geomechanics* 37(12)
376 1737–1760.

377 Zhang QY, Chen WW, Zhang YM. (2019). Modification and evaluation of Green–Ampt model:
378 Dynamic capillary pressure and broken-line wetting profile. *Journal of Hydrology* 575
379 1123-1132.

380 Zhu SR, Wu LZ, Peng JB. (2020). An improved Chebyshev semi-iterative method for
381 simulating rainfall infiltration in unsaturated soils and its application to shallow landslides.
382 *Journal of Hydrology* 125157.

383

384 **Captions of Tables and Figures**

385 **Table 1** Calculation parameters of Case 1

386 **Table 2** Calculation parameters of Case 2

387 **Table 3** Calculation parameters of Case 3

388 **Fig. 1** Infiltration in a soil slope during rainfall

389 **Fig.2** Infiltration behavior of water in the soil

390 **Fig.3** The flow chart of the proposed model

391 **Fig.4** The calculation results of Case 1: (a) rainfall intensity and infiltration rate of water in
392 soils, (b) the wetting front vs. time curve, and (c) the safety factor during rainfall

393 **Fig.5** Results of the proposed model and Eq. (14)

394 **Fig.6** The calculation results of Case 2: (a) rainfall intensity and infiltration rate of water in soil,
395 (b) the wetting front depth vs. time curve, and (c) the safety factor during rainfall

396 **Fig.7** The calculation results of Case 3: (a) rainfall intensity and infiltration rate of water in soil,
397 (b) the wetting front depth vs. time curve, and (c) the safety factor during rainfall

398 **Fig.8** Samples of saturated permeability coefficient

399 **Fig.9** (a) Wetting front depth-time curve and (b) safety factor-time curve

400 **Fig. 10** Slope failure probability during rainfall